Residual Stress and Fracture Analysis of Thick Plate for Partial Penetration Multi-Pass Weldment

Seok Kim
Defence Quality Assurance Agency, Seoul 130-010, Korea
Yong Lae Shim
Department of Welding Engineering, The Ohio State University, Ohio 43210, USA
Jung Il Song*
Department of Mechanical Engineering, Changwon National University, Kyungnam 641-773, Korea

Partial penetration welding joint refers to the groove weld that applies to the one side welding which does not use steel backing and to both side welding without back gouging, that is, the partial penetration welding joint leaves an unwelded portion at the root of the welding area. In this study, we analyzed the residual stress and fracture on the thick metal plates that introduced the partial penetration welding method. According to the above-mentioned welding method, we could draw a conclusion that longitudinal stress and traverse stress occurred around the welding area are so minimal and do not affect any influence. We also performed the fracture behavior evaluation on the partial penetration multi pass welding with 25.4 mm thick plate by using the J-integral, which finally led us the conclusion that the partial penetration multi-pass welding method is more applicable and effective in handling the root face with less than 6.35 mm.

Key Words: Partial Penetration Welding, Multi-Pass Weld, Residual Stress, $\hat{J}$-integral, Fracture

1. Introduction

The multi-pass weldment of thick plate adopts full penetration which has a superior strength. But full penetration needs excessive welding procedure and materials and there may exist a possibility of welding deformation and high residual stress. The partial penetration welding is adopted for the latest large combat vehicles in order to prevent above-mentioned problems in welding structures, and it is said to be good for the productivity, cost reduction, and automation. Partial penetration weldment is defined as the welding joint which includes unwelded part without back gouging.

The omission of back gouging, which is characteristics of partial penetration, makes automatic welding possible, and there is an example of 33% automatic welding by use of partial penetration on M1A1 vehicle of GDLS. The reason why partial penetration is not used widely in spite of great merit of automation is becaeese it has an unwelded part, which is not permissible in full penetration and expected to cause a deteriorating effect to strength and safety of structure. Therefore, the adoption of partial penetration requires a pre-study on structural strength and fracture feature.

The tensile residual stress in a welded part increases cracking and reduces the fracture resistance, which has a great effect to the fracture behavior (Masubuchi, 1980). The prediction of residual stress and accurate understanding of the

* Corresponding Author,
E-mail : jisong@sarim.changwon.ac.kr
TEL : +82-55-279-7508; **FAX** : +82-55-275-0101
Department of Mechanical Engineering, Changwon National University, Kyungnam 641-773, Korea. (Manuscript **Received** June 5, 2001; **Revised** May 27, 2002)

effect of residual stress on the fracture behavior is very important for the estimation of safety and durability of structure. In general, the numerical analysis using FEM is used for the prediction of residual stress distribution rather than the experimental method (Tall, 1964; Masubuchi, 1974; Fujita and Nomoto, 1972; Ueda and Yamakawa, 1973; Yasuhisa, 1996).

The path independency regardless of J-integral (Rice, 1968) of weldment is lost by residual stress (Kishimoto et al., 1980; Aoki et al., 1982; Wilson et al., 1979). Therefore, the analysis method making allowance for the plastic deformation of weldment is necessary for the understanding of fracture feature. Kishimoto et al. (1980), proposed the $\hat{J}$-integral which is applicable for analyzing the combined stress including thermal stress, and Shim (1997) applied it to the analysis of residual stress and plastic deformation. The residual stress distribution analysis using FEM of partial penetration multi-pass weldment and the analysis of fracture feature per RF(Root Face) size by residual stress analysis and $\hat{J}$-integral are performed in this study.

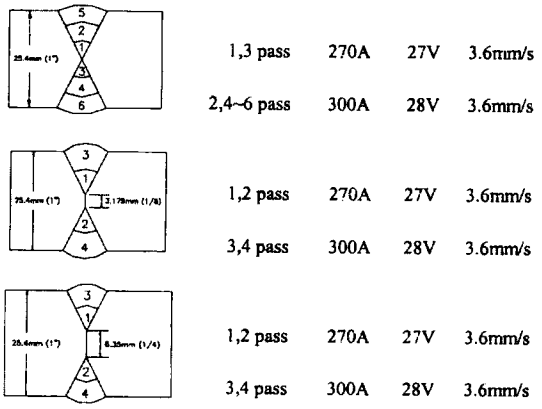

Fig. 1 Penetration shape and welding parameter

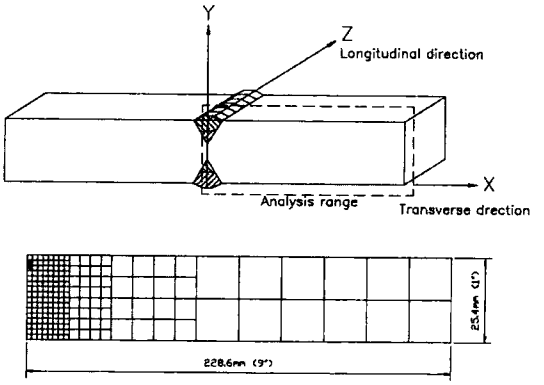

Fig. 2 FEM model of partial penetration weldment

2. Residual Stress Analysis

2.1 FEM analysis model

The thick plate is welded by welding base material at room temperature without preheating and cooling down to room temperature and next pass welding is done. Therefore two dimensional analysis of a section perpendicular to welded pass was performed with assumption that each section has same variation of temperature (Shim and Lee, 1993). The heat input into two dimensional element is calculated by the heat input per unit area given by

$$q=\frac{\eta EI}{bL} \tag{1}$$

Here, η denotes the welding efficiency, E the voltage, I the ampere, B the bead width, L the welded length, and L means unit length under the assumption of two dimensional element.

The welding model of this study is 25.4 mm thick plate which is most widely used for combat vehicle structures and full and partial penetration weldment of GMAW are compared. Six pass welding is applied to full penetration, and 6.35 mm (RF1/4) and 3.18 mm (RF1/8) welding are applied to partial penetration. And, the length 228.6 mm (9inch) equals to that of specimens. The welding shape and condition are presented in Fig. 1. FEM analysis model is shown in Fig. 2.

ABAQUS (2000) is used for the thermal residual stress analysis is done with the selection of 8 node plane element. Weld bead elements were deactivated at the initial stage and next activated according to each weld sequence. Initial temperature is assumed to be room temperature (21℃). The residual stress experiment for each weldment was performed by hole drilling method (ASTM, 1994) and measured at the distance 17.8 mm (0.7 inch), 25.4 mm (1 inch), 50.8 mm (2 inh) from the welding centerline with strain gage. The

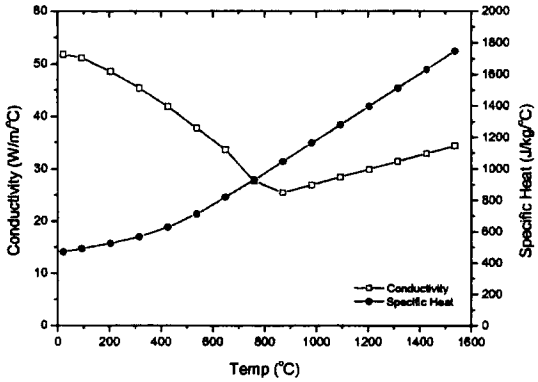

Fig. 3 Conductivity and specific heat of ASTM A36 steel

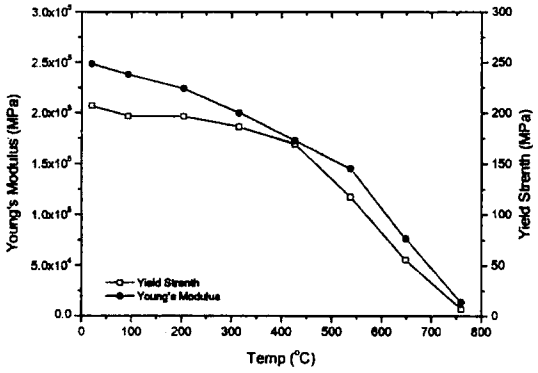

Fig. 4 Mechanical properties of ASTM A36 steel

material used for analysis and experiment is ASTM A36 and its properties are given in Fig. 3 and Fig. 4.

2.2 Results of analysis

The longitudinal residual stress (σ_{zz}) distributions at the top surface of partial and full penetration are compared in Fig. 5. According to Fig. 5, the residual stress distribution of RF1/4, RF1/8 partial penetration has a tendency to move toward the centerline compared with that of full penetration. The error between the analysis by ABAQUS and the measurement by strain gage is within 10%. From the experiment measurement at distance 17.8 mm from centerline shows that the stress of full penetration is 9% higher than that of RF1/4 partial penetration and 30% higher than that of RF1/8 partial penetration. And the stress measured at distance 25.4 mm from centerline of

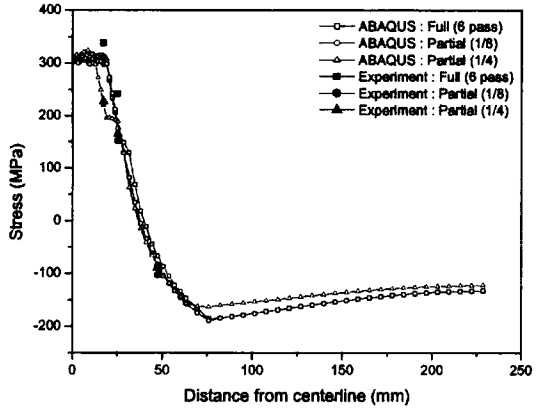

Fig. 5 Longitudinal residual stress (σ_{zz}) distribution at the top surface

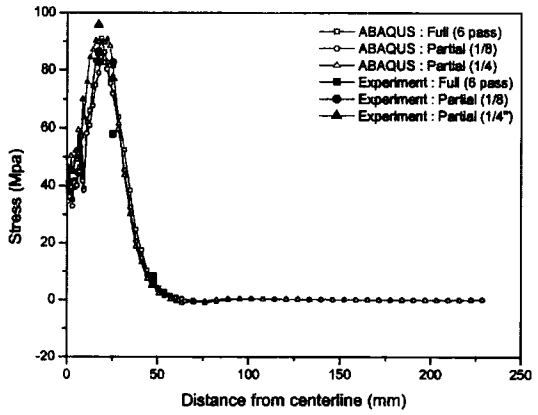

Fig. 6 Transverse residual stress (σ_{xx}) distribution at the top surface

full penetration is 46% higher than that of partial penetration. From this results, the partial penetration has less residual stress than full penetration by reduction of welding pass.

The transverse residual stress (σ_{xx}) distribution at the top surface is shown in Fig. 6. This confirms the analysis accuracy by ABAQUS within 12% error. According to the analysis by ABAQUS show in Fig. 6, there is almost no difference in transverse residual stress (σ_{xx}) between partial and full penetration. From this result, the partial penetration is not expected to have an influence on transverse residual stress (σ_{xx}) distribution.

The transverse-through-thickness residual stress (σ_{xx}) distribution is shown in Fig. 7. It

shows that both partial and full penetration produce tensile stress at top surface, and compressive stress at base surface, and there are three stress slopes along thickness. But the partial penetration differs from full penetration in that there is a large stress difference at 12.7 mm thickness (unwelded part) at which compressive stress crosses and more difference at RF1/4. This is expected to happen by the deflation resulted from thermal deformation of unwelded part during welding. The longitudinal-through-thickness residual stress (σ_{zz}) distribution is shown in Fig. 8. The stress distribution is similar to that of transverse residual stress (σ_{xx}) presented in Fig. 7, where both full and partial penetration have very high tensile stress.

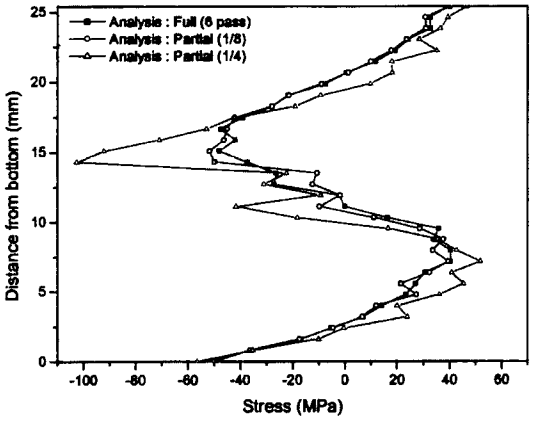

Fig. 7 Transverse through-thickness residual stress (σ_{xx}) distribution

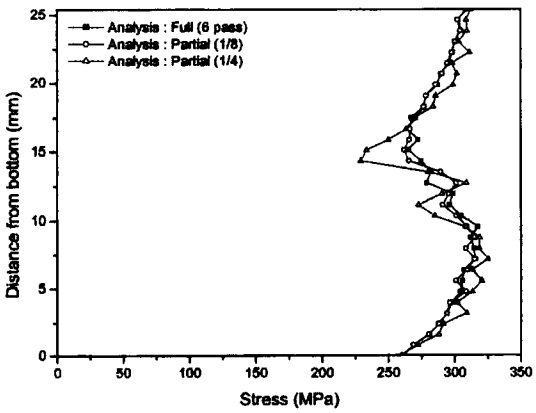

Fig. 8 Longitudinal through-thickness residual stress (σ_{zz}) distribution

3. Fracture Analysis

3.1 The theory of $\hat{J}$-integral

$\hat{J}$-integral means the rate of the energy change of the material in the fracture process region where continuum mechanics do not work which was derived by Kishimoto et al. (1980), based upon energy conservation principle,

$$\sigma_{ij,j}+F_i=\rho\ddot{u}_i \tag{2}$$

$\hat{J}$-integral is expressed like Eq. (3) provided crack tip and fracture process region are given in Fig. 9.

$$\hat{J}=-\int_{\Gamma_{end}} T_i\frac{\partial u_i}{\partial x_1}d\Gamma \tag{3}$$

Here, σ_{ij} denotes stress tensor, T_i the surface tensile force, u_i the displacement, A_{end} the fracture process region, and Γ_{end} means integral path which encloses A_{end}.

Eq. (3) can be expressed like follows.

$$\hat{J}=\int_{\Gamma+\Gamma_1-\Gamma_{end}} T_i\frac{\partial u_i}{\partial x_1}d\Gamma-\int_{\Gamma+\Gamma_1} T_i\frac{\partial u_i}{\partial x_1}d\Gamma \tag{4}$$

The right terms of Eq. (4) are summarized like Eq. (5) by the divergence theorem :

$$\hat{J}=\int_A\left(\sigma_{ij}\frac{\partial\varepsilon_{ij}}{\partial x_1}\right)_{,j}dA-\int_{\Gamma+\Gamma_1} T_i\frac{\partial u_i}{\partial x_1}d\Gamma \tag{5}$$

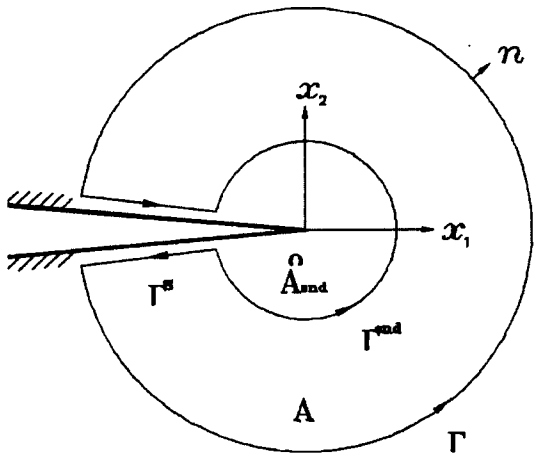

Fig. 9 Configuration of crack tip and fracture process region

And the Eq. (5) is summarized like Eq. (8) by the use of Eq. (2) of energy balance equation, strain Eq. (6) including plastic deformation by external load and welding heat and Eq. (7) of strain energy density :

$$\varepsilon_{ij}=\varepsilon_{ij}^{e}+\varepsilon_{ij}^{p}+\varepsilon_{ij}^{ip} \tag{6}$$

$$W_e(\varepsilon_{ij}^{e})=\int_0^{\varepsilon_{ij}}\sigma_{ij}d\varepsilon_{ij} \tag{7}$$

$$\hat{\mathrm{J}}=\int_A\{\,W_{e,1}-\sigma_{ij}u_{i,1}+\sigma_{ij}(\varepsilon_{ij}^{p}+\varepsilon_{ij}^{ip})\}dA \tag{8}$$

Here, ε_{ij}^{p} denotes plastic strain from mechanical loads cand ε_{ij}^{ip} is initial plastic strain after welding Eq. (8) must be transformed into FEM calculating form. Eq. (8) is expressed like Eq. (9) by the use of smooth function q, which has unit value at Γ_{end} and zero at Γ :

$$\hat{\mathrm{J}}=\int_A\left\{\frac{\partial W_e}{\partial x_1}q-\sigma_{ij}\frac{\partial u_i}{\partial x_1}q_{,i}+\sigma_{ij}\frac{\partial(\varepsilon_{ij}^{p}+\varepsilon_{ij}^{ip})}{\partial x_1}q\right\}dA \tag{9}$$

Eq. (9) is transformed into FEM form when D is Jacobian matrix, w is weight factor ;

$$\hat{\mathrm{J}}=\sum_{Elem}\sum_{Gauss}\left[\frac{\partial W_e}{\partial x_1}q-\sigma_{ij}\frac{\partial u_i}{\partial x_1}q_{,i}+\sigma_{ij}\frac{\partial(\varepsilon_{ij}^{p}+\varepsilon_{ij}^{ip})}{\partial x_1}q\right]\cdot Dw \tag{10}$$

$\hat{\mathrm{J}}$-integral program is made of FORTRAN by use of Eq. (10). $\hat{\mathrm{J}}$-integral is calculated by inputting the stress, strain energy density, plastic strain by external load and welding heat and node displacement of element.

3.2 Calculation result

3.18 mm (1/8 inch) crack tip was applied to the top surface where tensile residual stress acts after stress analysis by ABAQUS and $\hat{\mathrm{J}}$-integral was calculated by seven integral paths. The shape at the crack tip is depicted in Fig. 10.

The $\hat{\mathrm{J}}$-integral was performed for residual stress without external load and for residual stress with external load of 68.9 MPa (10 ksi), 137.9 MPa (20 ksi), 206.8 MPa (30 ksi), 275.8 MPa (40 ksi). The $\hat{\mathrm{J}}$-integral values of pull penetration is presented in Fig. 11.

The first path of $\hat{\mathrm{J}}$-integral has a singular point, but the integral values after that path are nearly constant. The reason why there occurs a singular point at first path is expected to be that the stress concentration by external load and large plastic

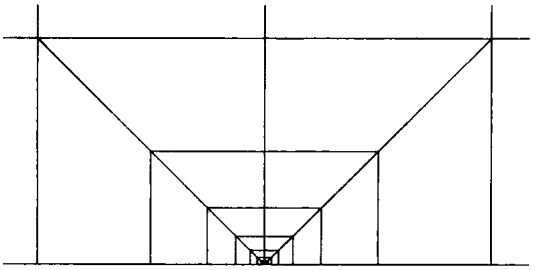

Fig. 10 The shape at the crack tip

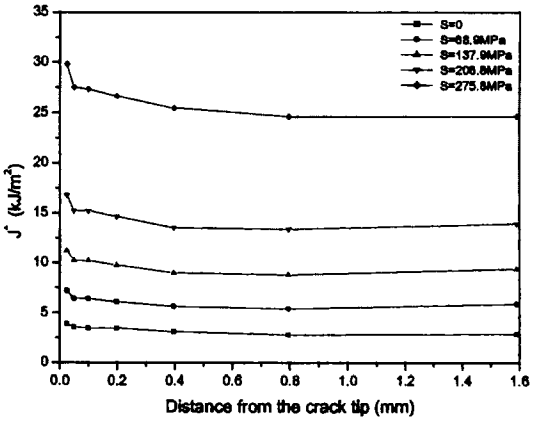

Fig. 11 The $\hat{\mathrm{J}}$-integral values of full penetration joint for combined residual stress and external loads

deformation by concentration has happened to the first path which has very small crack element. The $\hat{\mathrm{J}}$-integral value of no external load shows 2.88 kJ/m^2 (16.45 psi-in) at final integral path, which is equivalent to the case of external load of 159.5 MPa (23.13 ksi) without residual stress. According to Fig. 11, $\hat{\mathrm{J}}$-integral value increases gradually as external load increases from 68.9 MPa (10 ksi) to 206.8 MPa (30 ksi), but there is a rapid increase after 275.8 MPa (40 ksi).

Figure 12 shows the $\hat{\mathrm{J}}$-integral value for RF 1/8 partial penetration joint. There is also a singular point at first path but nearly constant after that path. Figure 12 shows the $\hat{\mathrm{J}}$-integral value of no external load is 2.85 kJ/m^2 (16.28 psi-in) at final integral path, which is equivalent to the case of external load of 156.9 MPa (22.75 ksi) without residual stress. The comparison between Fig. 11 and Fig. 12 shows that the $\hat{\mathrm{J}}$-integral values of RF1/8 partial penetration are a little

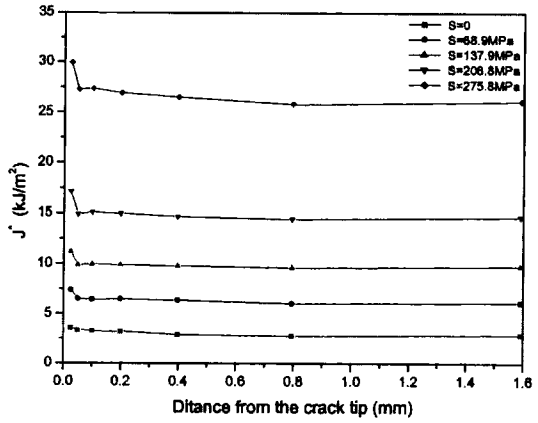

Fig. 12 The $\hat{J}$-integral values for the RF1/8 partial penetration joint for combined residual stress and external loads

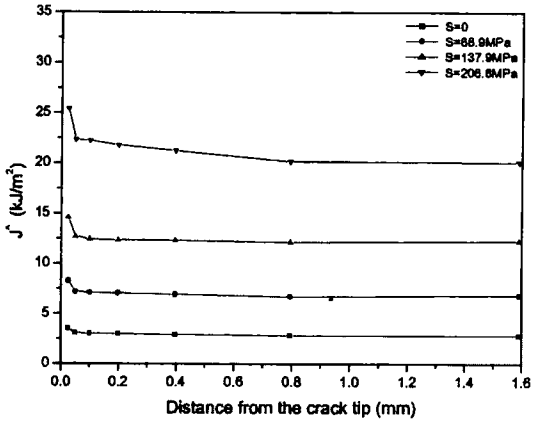

Fig. 13 The $\hat{J}$-integral values of the RF1/4 partial penetration joint for combined residual stress and external loads

higher than those of full penetration under the same external load.

Figure 13 shows the $\hat{J}$-integral value for RF 1/4 partial penetration joint. The $\hat{J}$-integral values are similar to those of Fig. 11 and Fig. 12 but shows higher values for the same external load. Figure 13 shows the $\hat{J}$-integral value of no external load is 2.82 kJ/m^2 (16.12 psi-in) at final integral path, which is equivalent to the external load of 145.7 MPa (21.13 ksi) and there is a rapid increase after 206.8 MPa (30 ksi). The $\hat{J}$-integral values of Fig. 11~Fig. 13 are compared in Fig. 14. As shown in Fig. 14, the $\hat{J}$-integral values for residual stress without external

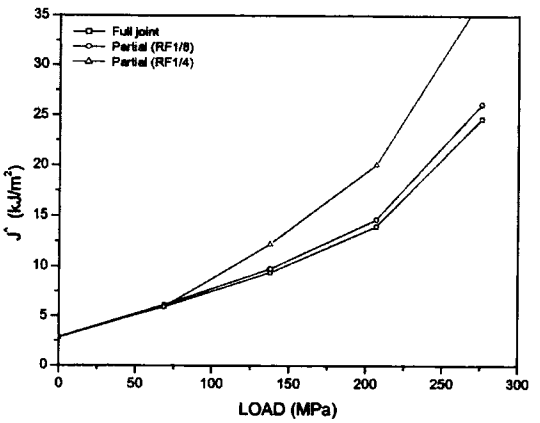

Fig. 14 The $\hat{J}$-integral values of full and partial penetration joint for combined residual stress and external loads

load are generally similar for both partial and full penetration joint. But with the increase of external load, the $\hat{J}$-integral values of RF1/8 partial penetration are about 3~5% higher than those of full penetration joint. And the $\hat{J}$-integral values of RF1/4 partial penetration shows a rapid increase after external load of 68.9 MPa (10 ksi), and 44% higher than full penetration at 206.8 MPa (30 ksi).

4. Conclusion

Under the full and partial penetration multi-ass weldment for the 25.4 mm thick plate the conclusions resulted from the fracture analysis by residual stress and $\hat{J}$-integral method using ABAQUS are as follows.

(1) Concerning longitudinal residual stress (σ_{zz}) distribution at the top surface, there is less residual stress in partial penetration than full penetration by the number of welding pass. But the transvers residual stress (σ_{xx}) distribution is not influenced by both partial and full penetration.

(2) Concerning transvers residual stress (σ_{xx}) at the through thickness, there is a stress variation at unwelded part of partial penetration at which the tensile and compressive stress crosses. But longitudinal residual stress (σ_{zz}) distribution of partial and full penetration is similar and both

have high tensile stress.

(3) The $\hat{J}$-integral value of 25.4 mm thick plate for full penetration multi-ass weldment shows 2.88 kJ/m^2 (16.45 psi-in) at final integral path when there is no external load, which is equivalent to the case of external load of 159.5 MPa (23.13 ksi) without residual stress. And the $\hat{J}$-integral value for both RF4/1 and RF1/8 are similar to those of full penetration.

(4) The $\hat{J}$-integral values of RF1/8 partial penetration are 3~4% higher than those of full penetration when there is a combined stress of external load and residual stress.

(5) The $\hat{J}$-integral values of RF1/4 partial penetration are similar to those of full penetration and RF1/8 partial penetration, but there is a rapid increase after external load of 68.9 MPa (10 ksi) unlike them. Therefore, root face smaller than 6.35 mm (1/4 inch) should be used for partial penetration welding for the consideration of fracture behavior of weldment.

References

ABAQUS User's Manual, 2000, HKS inc.

ASTM E837-94, "Standard Test Method for Determining Residual Stresses by the Hole Drilling Strain Gage Method."

AWS D1. 1 Structural Welding Code.

Aoki, S., Kishimoto, K. and Sakata, M., 1982, "Elastic-Plastic Analysis of Crack in Thermally Loaded Structures," *Engineering Fracture Mechanics*, Vol. 16, No. 3, pp. 405~413.

Fujita, Y. and Nomoto, T., 1972, "Studies on Thermal Elasto-Plastic Problems," *Journal of the Society of Naval Architects of Japan*, Vol. 130.

Kishimoto, K., Aoki, S. and Sakata, M., 1980, "On the Path Independent Integral," *Engineering Fracture Mechanics*, Vol. 13, pp. 841~850.

Masubuchi, K., 1980, "Analysis of Welded Structures," Pergamon Press, p. 148.

Masubuchi, K., 1974, "Analysis of Thermal Stresses and Metal Movements of Weldments : A Basic Study toward Computer Aided Analysis and Control of Welded Structure," *SNAME Trans.*, Vol. 82, pp. 143~167.

Rice, J. R., 1968, "A Path Independent Integral and the Approximate Analysis of Strain Concentration by Notches and Crack," *Journal of Applied Mechanics*, Vol. 35, pp. 379~386.

Shim, Y. L. and Lee, S. G., 1993, "Modeling of Welding Heat Input for Residual Stress Analysis," *Journal of the Korean Welding Society*, No. 3, p. 112.

Shim, Y. L., 1997, "Residual Stress, Distortion, and Fracture Analysis of Welded Structures using Finite Element Method," *Journal of* KWS, Vol. 15, No. 2, pp. 15~25.

Tall, L., 1964, "Residual Stresses in Welded Plates-A Theoretical Study," *Welding Journal*, Vol. 43.

Ueda, Y. and Yamakawa, T., 1973, "Analysis of Thermal Elasto-Plastic Behavior of Metals during Welding by Finite Element Method," *Journal of the Japanese Welding Society*, Vol. 42, No. 6.

Wilson, W. K. and Yu, I. W., 1979, "The Use of the J-integral in Thermal Stress Crack Problems," *International Journal of Fracture*, Vol. 15, No. 4, pp. 377~387.

Yasuhisa, O., 1996, "Simulation of Welding Deformation by FEM," *TEAM '96 PUSAN*, pp. 593~605.